Detecting small-scale spatial heterogeneity and temporal dynamics of soil organic carbon (SOC) stocks: a comparison between automatic chamber-derived C budgets and repeated soil inventories

Mathias Hoffmann[a,*], Nicole Jurisch[b], Juana Garcia Alba[a], Elisa Albiac Borraz[a], Marten Schmidt[b], Vytas Huth[b], Helmut Rogasik[a], Helene Rieckh[a], Gernot Verch[c], Michael Sommer[a, d], Jürgen Augustin[b]

[a]Institute of Soil Landscape Research, Leibniz Centre for Agricultural Landscape Research (ZALF), Eberswalder Str. 84, 15374 Müncheberg, Germany

[b]Institute of Landscape Biogeochemistry, Leibniz Centre for Agricultural Landscape Research (ZALF), Eberswalder Str. 84, 15374 Müncheberg, Germany

[c]Research Station Dedelow, Leibniz Centre for Agricultural Landscape Research (ZALF), Eberswalder Str. 84, 15374 Müncheberg, Germany

[d]Institute of Earth and Environmental Sciences, University Potsdam, Karl-Liebknecht-Str.24-25, 14476 Potsdam, Germany

*Corresponding author:

Mathias Hoffmann

Eberswalder Str. 84, 15374 Müncheberg, Germany

E-mail: Mathias.Hoffmann@zalf.de

Tel.: +49(0)33432 82 4068

Fax: +49(0)33432 82 280

Abstract

Carbon (C) sequestration in soils plays a key role in the global C cycle. It is therefore crucial to adequately monitor dynamics in soil organic carbon (ΔSOC) stocks when aiming to reveal underlying processes and potential drivers. However, small-scale spatial (10-30 m) and temporal changes in SOC stocks, particularly pronounced on arable lands, are hard to assess. The main reasons for this are limitations of the well-established methods. On the one hand, repeated soil inventories, often used in long-term field trials, reveal spatial patterns and trends in ΔSOC but require a longer observation period and a sufficient number of repetitions. On the other hand, eddy covariance measurements of C fluxes towards a complete C budget of the soil-plant-atmosphere system may help to obtain temporal ΔSOC patterns but lack small-scale spatial resolution.

To overcome these limitations, this study presents a reliable method to detect both short-term temporal dynamics as well as small-scale spatial differences of ΔSOC using measurements of the net ecosystem carbon balance (NECB) as a proxy. To estimate the NECB, a combination of automatic chamber (AC) measurements of CO_2 exchange and empirically modeled aboveground biomass development (NPP_{shoot}) were used. To verify our method, results were compared with ΔSOC observed by soil resampling.

Soil resampling and AC measurements were performed from 2010 to 2014 at a colluvial depression located in the hummocky ground moraine landscape of NE Germany. The measurement site is characterized by a variable groundwater level (GWL) and pronounced small-scale spatial heterogeneity regarding SOC and nitrogen (Nt) stocks. Tendencies and magnitude of ΔSOC values derived by AC-measurements and repeated soil inventories corresponded well. The period of maximum plant growth was identified as being most important for the development of spatial differences in annual ΔSOC. Hence, we were able to confirm that AC-based C budgets are able to reveal small-scale spatial differences and short-term temporal dynamics of ΔSOC.

Keywords

Net ecosystem exchange (NEE), net primary productivity (NPP), biomass modeling, soil resampling

1. Introduction

Soils are the largest terrestrial reservoirs of organic carbon (SOC), storing two to three times as much C as the atmosphere and biosphere (Chen et al., 2015; Lal et al., 2004). In the context of climate change mitigation as well as soil fertility and food security, there has been considerable interest in the development of SOC, especially in erosion-affected agricultural landscapes (Berhe and Kleber, 2013; Conant et al., 2011; Doetterl et al., 2016; Stockmann et al., 2015; Van Oost et al., 2007; Xiong et al., 2016). Detecting the development of soil organic carbon stocks (ΔSOC) in agricultural landscapes needs to consider three major challenges: First, the high small-scale spatial heterogeneity of SOC (e.g., Conant et al., 2011; Xiong et al., 2016). Erosion and land use change reinforce natural spatial and temporal variability, especially in hilly landscapes such as hummocky ground moraines where correlation lengths in soil parameters of 10-30 m are very common. Second, pronounced short-term temporal dynamics, caused by, e.g., type of cover crop, frequent crop rotation and soil cultivation practices. Third, the rather small magnitude of ΔSOC compared to total SOC stocks (e.g., Conant et al., 2011; Poeplau et al., 2016).

However, information on the development of SOC is an essential precondition to improve the predictive ability of terrestrial C models (Luo et al., 2014). As a result, sensitive measurement techniques are required to precisely assess short-term temporal and small-scale (10-30 m) spatial dynamics in ΔSOC (Batjes and van Wesemael, 2015). To date, the assessment of ΔSOC is typically based on two methods, namely (i) destructive, repeated soil inventories through soil resampling and (ii) non-destructive determination of ecosystem C budgets (NECB) by measurements of gaseous C exchange, C import and C export (Leifeld et al., 2011; Smith et al., 2010).

The first method is usually used during long-term field trials (Batjes and van Wesemael, 2015; Chen et al., 2015; Schrumpf et al., 2011). Given a sufficient time horizon of 5 to 10 years, the soil resampling method is generally able to reveal spatial patterns and trends within ΔSOC (Batjes and

van Wesemael, 2015; Schrumpf et al., 2011). Most repeated soil inventories are designed to study treatment differences in the long-term. As a result, short-term temporal dynamics in C exchange remain concealed (Poeplau et al., 2016; Schrumpf et al., 2011). A number of studies tried to overcome this methodical limitation by increasing (e.g., monthly) the soil sampling frequency (Culman et al., 2013; Wuest, 2014). This allows for the detection of seasonal patterns of ΔSOC but still mixes temporal and spatial variability of SOC because every new soil sample represents not only a repetition in time but also in space. Temporal differences observed through repeated soil sampling are therefore always spatially biased.

By contrast, the NECB (Smith et al. 2010) - used as a proxy for temporal dynamics of ΔSOC - can be easily derived through the eddy covariance (EC) technique, representing a common approach to obtain gaseous C exchange (Alberti et al., 2010; Leifeld et al., 2011; Skinner and Dell, 2015). However, C fluxes based on EC measurements are integrated over a larger, altering footprint area (several hectares). As a result, small-scale (< 20 m) spatial differences in NECB and ΔSOC are not detected.

Accounting for the above-mentioned methodical limitations, a number of studies investigated spatial patterns in gaseous C exchange by using manual chamber measurement systems (Eickenscheidt et al., 2014; Pohl et al., 2015). Compared to EC measurements, these systems are characterized by a low temporal resolution, where the calculated net ecosystem CO_2 exchange (NEE) is commonly based on extensive gap filling (Gomez-Casanovas et al., 2013; Savage and Davidson, 2003) conducted, e.g., using empirical modeling (Hoffmann et al., 2015). Therefore, management practices and different stages in plant development that are needed to precisely detect NEE often remain unconsidered (Hoffmann et al., 2015).

Compared to mentioned approaches for detecting ΔSOC by either repeated soil sampling or observations of the gaseous C exchange (NECB), automatic chamber (AC) systems combine

several advantages. On the one hand flux measurements of the same spatial entity avoid the mixing of spatial and temporal variability, as done in case of point measurements by repeated soil inventories. On the other hand, AC measurements combine advantages of EC and manual chamber systems because they not only increase the temporal resolution compared to manual chambers but also allow for the detection of small-scale spatial differences and treatment comparisons regarding the gaseous C exchange (Koskinen et al., 2014).

To date hardly any direct comparisons between AC-derived C budgets and soil resampling-based ΔSOC values have been reported in the literature. Leifeld et al. (2011) and Verma et al. (2005) compared the results of repeated soil inventories with EC-based C budgets over 5- and 3-year study periods, respectively. Even though temporal dynamics in ΔSOC were shown e.g. for grazed pastures and intensively used grasslands (Skinner and Dell 2015; Leifeld et al., 2011), no attempt was made to additionally detect small-scale differences in ΔSOC. In our study, we introduce the combination of AC measurements and empirically modeled aboveground biomass production (NPP_{shoot}) as a precise method to detect small-scale spatial differences and short-term temporal dynamics of NECB and thus ΔSOC. Measurements were performed from 2010 to 2014 under a *silage maize/winter fodder rye/sorghum-Sudan grass hybrid/alfalfa* crop rotation at an experimental plot located in the hummocky ground moraine landscape of NE Germany.

We hypothesize that the AC-based C budget method is able to detect small-scale spatial and short-term temporal dynamics of NECB and thus ΔSOC in an accurate and precise manner. Therefore, we compare ΔSOC values measured by soil resampling with NECB values derived through AC-based C budgets (Fig. 1).

2. Materials and methods

2.1 Study site and experimental setup

Measurements were performed at the 6-ha experimental field "CarboZALF-D". The site is located in a hummocky arable soil landscape within the Uckermark region (NE-Germany; 53°23`N, 13°47`E, ~50-60 m a.s.l.). The temperate climate is characterized by a mean annual air temperature of 8.6°C and annual precipitation of 485 mm (1992–2012, ZALF research station, Dedelow). Typical landscape elements vary from flat summit and depression locations with a gradient of approximately 2 %, across longer slopes with a medium gradient of approx. 6 %, to short and rather steep slopes with a gradient of up to 13 %. The study site shows complex soil patterns mainly influenced by erosion, relief and parent material, e.g., sandy to marly glacial and glaciofluvial deposits. The soil type inventory of the experimental site consists of non-eroded Albic Luvisols (Cutanic) at the flat summits, strongly eroded Calcic Luvisols (Cutanic) on the moderate slopes, extremely eroded Calcaric Regosols on the steep slopes, and a colluvial soil, i.e., Endogleyic Colluvic Regosols (Eutric), over peat in the depression (IUSS Working Group WRB, 2015).

During June 2010, four automatic chambers and a WXT520 climate station (Vaisala, Vantaa, Finland) were set up at the depression (Sommer et al., 2016) (see 2.2.1). The chambers were arranged along a topographic gradient (upper (A), upper middle (B), lower middle (C), and lower (D) chamber position; length ~30 m; difference in altitude ~1 m) within in a distance of approx. 5 m of each other (Fig. 2). As part of the CarboZALF project, a manipulation experiment was carried out at the end of October 2010, i.e., after the vegetation period (Deumlich et al., 2017). Topsoil material from a neighboring hillslope was incorporated into the upper soil layer of the depression (Ap horizon). The amount of translocated soil was equivalent to tillage erosion of a decennial time horizon (Sommer et al., 2016). The change in SOC for each chamber was monitored by three topsoil inventories, carried out (I) prior to soil manipulation during April 2009, (II) after soil manipulation during April 2011, and (III) during December 2014. ΔSOC derived through soil

resampling and AC-based C budgets (NECB), was compared for the period between April 2011 and December 2014 (Fig. 1).

Records of meteorological conditions (1 min frequency) include measurements of air temperature at 20 cm and 200 cm height, PAR (inside and outside the chamber), air humidity, precipitation, air pressure, wind speed and direction. Soil temperatures at depths of 2 cm, 5 cm, 10 cm and 50 cm were recorded using thermocouples, installed next to the climate station (107, Campbell Scientific, UT, USA).

The groundwater level (GWL) was measured using tensiometers assuming hydrostatic equilibrium. The tensiometers were installed at a soil depth of 160 cm, at soil profile locations in the upper and lower end of the transect. The average GWL of both profiles was used for further data analysis. Data gaps < 2 days were filled using simple linear interpolation. Larger gaps in GWL did not occur.

The measurement site was cultivated with five different crops during the study period, following a practice-orientated and erosion-expedited farming procedure. The crop rotation was silage maize (*Zea mays*) - winter fodder rye (*Secale cereale*) - sorghum-Sudan grass hybrid (*Sorghum bicolor* x *sudanese*) - winter triticale (*Triticosecale*) - alfalfa (*Medicago sativa*). Cultivation and fertilization details are presented in Tab. A.1. Aboveground biomass (NPP_{shoot}) development was monitored using up to four biomass sampling campaigns during the growing season, covering the main growth stages. Additional measurements of leaf area index (LAI) started in 2013. Collected biomass samples were chopped and dried to a constant weight (48 h at 105°C). The C, N, K and P contents were determined using elementary analysis (C, N: TruSpec CNS analyzer, LECO Ltd., Mönchengladbach, Germany) and Kjehldahl digestion (P, K; AT200, BeckmanCoulter (Olympus), Krefeld, Germany and AAS-iCE3300, ThermoFisher-SCIENTIFIC GmbH, Darmstadt, Germany). To assess the potential impact of chamber placement on plant growth, chemical analyses were

171 carried out for the final harvests of each chamber and compared to biomass samples collected next
172 to each chamber.
173
174 **2.2 C budget method**
175 **2.2.1 Automatic chamber system**
176 Automatic flow-through non-steady-state (FT-NSS) chamber measurements (Livingston and
177 Hutchinson, 1995) of CO_2 exchange were conducted from January 2010 until December 2014. The
178 AC system consists of 4 identical, rectangular, transparent polycarbonate chambers (thickness of 2
179 mm; light transmission ~70 %). Each chamber has a height of 2.5 m and covers a surface area of
180 2.25 m^2 (volume: 5.625 m^3). To adapt for plant height (alfalfa), the chamber volume was reduced
181 to 3.375 m^3 in autumn 2013. Airtight closure during measurements was ensured by a rubber belt
182 that sealed at the bottom of each chamber. A 30-cm open-ended tube on the slightly concave top
183 of the chambers guided rain water into the chamber and additionally assured pressure equalization.
184 Two small axial fans (5.61 m^3 min^{-1}) were used for mixing the chamber headspace. The chambers
185 were mounted onto steel frames with a height of 6 m and lifted between measurements using
186 electrical winches at the top. For controlling the AC system and data collection, a CR1000 data
187 logger was used (Campbell Scientific, UT, USA). The CO_2 concentration changes over time were
188 measured within each chamber using a carbon dioxide probe (GMP343, Vaisala, Vantaa, Finland)
189 connected to a vacuum pump (0.001 m^3 min^{-1}; DC12/16FK, Fürgut, Tannheim, Germany). All CO_2
190 probes were calibrated prior to installation using ± 0.5 % accurate gases containing 0 ppm, 200
191 ppm 370 ppm, 600 ppm, 1000, ppm and 4000 ppm CO_2. The operation schedule of the AC system,
192 decisively influenced by agricultural treatments, is presented in A.2. The chambers closed in
193 parallel at an hourly frequency, providing one flux measurement per chamber and hour. The
194 measurement duration was 5-20 minutes, depending on season and time of day. Nighttime

195 measurements usually lasted 10 min during the growing season and 20 min during the non-growing
196 season (due to lower concentration increments). The length of the daytime measurements was up
197 to 10 min, depending on low PAR fluctuations (< 20 %). CO_2 concentrations (inside the chamber)
198 and general environmental conditions, such as PAR (SKP215, Skye, Llandridad Wells, UK) and
199 air temperatures (107, Campbell Scientific, UT, USA), were recorded inside and outside the
200 chambers at a 1 min frequency from 2010 to 2012 and a 15 sec frequency from October 2012.
201
202 **2.2.2 CO_2 flux calculation and gap filling**
203 An adaptation of the modular R program script, described in detail by Hoffmann et al. (2015), was
204 used for stepwise data processing. The atmospheric sign convention was used for the components
205 of gaseous C exchange (ecosystem respiration (R_{eco}; sum of autotrophic and heterotrophic
206 respiration), gross primary production (GPP) and NEE), whereas positive values for NECB
207 indicate a gain and negative values a loss in SOC. Based on records of environmental variables and
208 CO_2 concentration change within the chamber headspace, CO_2 fluxes were calculated and
209 parameterized for R_{eco} and GPP within an integrative step. Subsequently, R_{eco}, GPP, and NEE were
210 modeled for the entire measurement period using climate station data. Statistical analyses, model
211 calibration and comprehensive error prediction were provided for all steps of the modeling process.
212 CO_2 fluxes (F, μmol C m^{-2} s^{-1}) were calculated according to the ideal gas law (Eq. 1).
213
214 $$F = \frac{pV}{RTA} * \frac{\Delta c}{\Delta t} \quad \text{[Eq. 1]}$$
215
216 where Δc/Δt is the concentration change over measurement time, A and V denote the basal area
217 and chamber volume, respectively, and T and p represent the air temperature inside the chamber
218 (K) and air pressure. Because plants below the chambers accounted for < 0.2 % of the total chamber

volume, a static chamber volume was assumed. R is a constant (8.3143 m^3 Pa K^{-1} mol^{-1}). To calculate $\Delta c/\Delta t$, data subsets based on a variable moving window with a minimum length of 4 minutes were used (Hoffmann et al., 2015). $\Delta c/\Delta t$ was computed by applying a linear regression to each data subset, relating changes in chamber headspace CO_2 concentration to measurement time (Leiber-Sauheitl et al., 2013; Leifeld et al., 2014; Pohl et al., 2015). In the case of the 15-sec measurement frequency, a death-band of 5 % was applied prior to the moving window algorithm. Thus, data noise that originated from either turbulence or pressure fluctuation caused by chamber deployment or from increasing saturation and canopy microclimate effects was excluded (Davidson et al., 2002; Kutzbach et al., 2007; Langensiepen et al., 2012). Due to the low measurement frequency, no data points were discarded for records with 1-min measurement frequency (2010-2012). The resulting CO_2 fluxes per measurement (based on the moving window data subsets) were further evaluated according to the following exclusion criteria: (i) range of within-chamber air temperature not larger than ± 1.5 K (R_{eco} and NEE fluxes) and a PAR deviation (NEE fluxes only) not larger than ± 20 % of the average to ensure stable environmental conditions within the chamber throughout the measurement; (ii) significant regression slope ($p \leq 0.1$, *t*-test); and (iii) non-significant tests ($p > 0.1$) for normality (Lillifor´s adaption of the Kolmogorov-Smirnov test), homoscedasticity (Breusch-Pagan test) and linearity of CO_2 concentration data. Calculated CO_2 fluxes that did not meet all exclusion criteria were discarded. In cases where more than one flux per measurement met all exclusion criteria, the CO_2 flux with the steepest slope was chosen.

To account for measurement gaps and to obtain cumulative NEE values, empirical models were derived based on nighttime R_{eco} and daytime NEE measurements following Hoffmann et al. (2015). For R_{eco}, temperature-dependent Arrhenius-type models were used and fitted for recorded air as well as soil temperatures in different depths (Lloyd and Taylor 1994; Eq. 2).

$$R_{eco} = R_{ref} * e^{E_0\left(\frac{1}{T_{ref}-T_0}-\frac{1}{T-T_0}\right)} \quad \text{[Eq. 2]}$$

where R_{eco} is the measured ecosystem respiration rate [µmol^{-1} C m^{-2} s^{-1}], R_{ref} is the respiration rate at the reference temperature (283.15 K; T_{ref}); E_0 is an activation energy like parameter; T_0 is the starting temperature constant (227.13 K) and T is the mean air or soil temperature during the flux measurement. Out of the four R_{eco} models (one model for air temperature, soil temperature in 2 cm, 5 cm and 10 cm depth) obtained for nighttime R_{eco} measurements of a certain period, the model with the lowest Akaike Information Criterion (AIC) was used.

GPP fluxes were derived using a PAR-dependent, rectangular hyperbolic light response function based on the Michaelis-Menten kinetic (Elsgaard et al., 2012; Hoffmann et al., 2015; Wang et al., 2013; Eq. 3). Because GPP was not measured directly, GPP fluxes were calculated as the difference between measured NEE and modeled R_{eco} fluxes.

$$GPP = \frac{GP_{max}*\alpha*PAR}{\alpha*PAR+GP_{max}} \quad \text{[Eq. 3]}$$

where *GPP* is the calculated gross primary productivity [µmol^{-1} CO_2 m^{-2} s^{-1}]; GP_{max} is the maximum rate of C fixation at infinite PAR [µmol CO_2 m^{-2} s^{-1}]; α is the light use efficiency [mol CO_2 mol^{-1} photons] and *PAR* is the photon flux density (inside the chamber) of the photosynthetically active radiation [µmol^{-1} photons m^{-2} s^{-1}]. In cases where the rectangular hyperbolic light response function did not result in significant parameter estimates, a non-rectangular hyperbolic light-response function was used (Gilmanov et al. 2007, 2013; Eq. 4).

$$GPP = \alpha * PAR + GP_{max} - \sqrt{(\alpha * PAR + GP_{max})^2 - 4 * \alpha * PAR * GP_{max} * \theta} \quad \text{[Eq. 4]}$$

where θ is the convexity coefficient of the light-response equation (dimensionless).

Due to plant growth and season, parameters of derived R_{eco} and GPP models may vary with time. To account for this, a moving window parameterization was performed, by applying fluxes of a variable time window (2-21 consecutive measurement days) to Eq.2-4. Temporally overlapping R_{eco} and GPP model sets were evaluated and discarded in case of positive (GPP), negative (R_{eco}) or insignificant parameter estimates. Finally, the model set with the lowest AIC (R_{eco}) was used. If no fit or a non-significant fit was achieved, averaged flux rates were applied for R_{eco} and GPP. The length of the averaging period was thereby selected by choosing the variable moving window with the lowest standard deviation (SD) of measured fluxes. This procedure was repeated until the whole study period was parameterized.

Based on continuously monitored temperature and PAR (outside the chamber), R_{eco}, GPP and NEE were modeled in half-hour steps for the entire study period. Because GPP was parameterized based on PAR records inside but modeled with PAR records outside the chamber, no PAR correction in terms of reduced light transmission was needed. Uncertainty of annual CO_2 exchange was quantified using a comprehensive error prediction algorithm described in detail by Hoffmann et al. (2015).

2.2.3 Modeling aboveground biomass dynamics

Aboveground biomass development (NPP_{shoot}) was predicted using a logistic empirical model (Yin et al., 2003; Zeide, 1993). From 2010 to 2012, modeled NPP_{shoot} was based on the relationship between sampling date and the C content of harvested dry biomass measured during sampling campaigns (three to four times per year following plant development). For alfalfa in 2013 and 2014,

290 NPP_{shoot} was modeled based on biweekly measurements of LAI because no additional biomass
291 sampling was performed between the multiple cuts per year. To calculate the C content
292 corresponding to the measured LAI, the relationship between LAI prior to the chamber harvest and
293 the C content measured in the chamber harvest of all six alfalfa cuts was used. Daily values of C
294 stored within NPP_{shoot} were calculated using derived logistic functions.
295
296 **2.2.4 Calculation of NECB**
297 Annual NECB for each chamber was determined as the sum of annual NEE and NPP_{shoot},
298 representing C removal due to the chamber harvest (Eq. 4; Leifeld et al., 2014). Temporal dynamics
299 in NECB were calculated as the sum of daily NEE and NPP_{shoot}.
300
301 $$NECB_n = \sum_{i=1}^{n}[NEE_i + CH_4 + (NPP_{shoot_i} - C_{import}) + \Delta DOC_i + \Delta DIC_i] \quad \text{[Eq. 5]}$$
302
303 Several minor components of Eq. 5 were not considered (see also Hernandez-Ramirez et al., 2011).
304 First, C import (C_{import}) due to seeding and fertilization, which was close to zero because the
305 measurement site was fertilized by a surface application of mineral fertilizer throughout the entire
306 study period. Second, methane (CH_4-C) emissions, which were measured manually at the same
307 experimental field but did not exceed a relevant order of magnitude (-0.01 g C m^{-2} y^{-1}) and were
308 therefore not included in the NECB calculation. Third, lateral C fluxes, originating from dissolved
309 organic (DOC) and inorganic carbon (DIC) as well as particulate soil organic carbon (SOC_p). In
310 addition to the rather small magnitude of the subsurface lateral C fluxes in soil solution (Rieckh et
311 al., 2012), it was assumed that their C input equaled C output at the plot scale. Lateral SOC_p
312 transport along the hillslope was excluded by grassland stripes established between experimental
313 plots in 2010 (Fig. 1 in Sommer et al., 2016).

2.3 Soil resampling method

To obtain ΔSOC using the soil resampling method, soil samples were collected three times during the study period. Initial SOC along the topographic gradient was monitored prior to soil manipulation during April 2009 at two soil pits, which were sampled by pedogenetic horizons. After soil manipulation, a 5-m raster sampling of topsoils (Ap horizons) was performed during April 2011. Each Ap horizon was separated into an upper (0-15 cm) and lower segment (15-25 cm), which were analyzed separately for bulk density, SOC, Nt and coarse fraction (< 2 mm) (data not shown). From these data, SOC and Nt mass densities were calculated separately for each segment and finally summed up for the entire Ap-horizon (0-25 cm). The mean SOC and Nt content for the Ap horizon of each raster point was calculated by dividing SOC or Nt mass densities (0-25 cm) through the fine-earth mass (0-25 cm). In December 2014, composite soil samples of the Ap horizon were collected. The composite samples consist of samples from four sampling points in a close proximity around each chamber. Prior to laboratory analysis coarse organic material was discarded from collected soil samples (Schlichting et al. 1995). Thermogravimetric desiccation at 105°C was performed in the laboratory for all samples to determine bulk densities (Mg m^{-3}). Bulk soil samples were air dried, gently crushed and sieved (2 mm) to obtain the fine fraction (particle size < 2 mm). The total carbon and total nitrogen contents were determined by elementary analysis (TruSpec CNS analyzer, LECO Ltd., Mönchengladbach, Germany) as carbon dioxide via infrared detection after dry combustion at 1250°C (DIN ISO10694, 1996), in duplicate. As the soil horizons did not contain carbonates, total carbon was equal to SOC.

2.4 Uncertainty prediction and statistical analysis

Uncertainty prediction for NECB derived by the C budget method was performed according to Hoffmann et al. (2015), following the law of error propagation. To test for differences in topsoil SOC (SOC_{Ap}) and total nitrogen (Nt) stocks between soil resampling performed after soil manipulation in 2010 and 2014, a paired *t*-test was applied. Computation of uncertainty prediction and calculation of statistical analyses were performed using R 3.2.2.

3. Results

3.1 C budget method

3.1.1 NEE and NPP_{shoot} dynamics

NEE and its components R_{eco} and GPP were characterized by a clear seasonality and diurnal patterns. Seasonality followed plant growth and management events (e.g., harvest; Fig. 3), Highest CO_2 uptake was thus observed during the growing season, whereas NEE fluxes during the non-growing season were significantly lower. Diurnal patterns were more pronounced during the growing season and less obvious during the non-growing season. In general R_{eco} fluxes were higher during daytime, whereas GPP and NEE, in case of present cover crops, were lower or even negative, representing a C uptake during daytime by the plant-soil system. Annual NEE was crop dependent, ranging from -1600 g C m^{-2} y^{-1} to -288 g C m^{-2} y^{-1}. Highest annual uptakes were observed for maize and sorghum during 2011 and 2012, whereas alfalfa cultivation showed lower annual NEE (Tab. 1). From 2010 to 2012, annual NEE followed the topographic gradient, with higher NEE in the direction of the depression and lower NEE away from the depression. These small-scale spatial differences in gaseous C exchange changed with alfalfa cultivation. As a result, only minor differences between the chamber positions were observed, showing no clear trend or tendency (Tab. 1).

C in living biomass (due to biomass sampling campaigns and LAI measurements) and C removals due to harvest were in general well reflected by modeled NPP_{shoot} (Fig. 4). Annual C removal due to harvest was clearly crop dependent, with highest NPP_{shoot} for maize and sorghum ranging from 420 g C m^{-2} to 1238 g C m^{-2}, and lower values in the case of winter fodder rye and alfalfa. Similar to NEE from 2010 to 2012, annual sums of NPP_{shoot} followed the topographic gradient, with lower values close to the depression (Tab. 1). Again, lower differences in annual NPP_{shoot} between the chambers and no spatial trends were found for alfalfa in 2013 and 2014.

3.1.2 NECB dynamics

Temporal and spatial dynamics of continously cumulated daily NECB values during the four years after soil manipulation are shown in Fig. 5. Differences in NECB were in general less pronounced during the non-growing season compared to the growing season. During the non-growing season, differences were mainly driven by differences in R_{eco} rather than GPP or NPP_{shoot}. This changed at the beginning of the growing season, when NECB responded to changes in cumulative NEE and NPP_{shoot}. Hence, up to 79 % of the standard deviation of estimated annual NECB developed during the period of maximum plant growth. Except for the lower middle chamber position, alfalfa seemed to counterbalance spatial differences in NECB that developed during previous years (Fig. 5).

Annual NECB values derived by the C budget method are presented in Tab. 1. Theron based highest annual SOC gains were obtained in 2012 for winter fodder rye and sorghum-Sudan grass, reaching an average of 474 g C m^{-2} y^{-1}. In contrast, maize cultivation during 2011 was characterized by C losses between 59 g C m^{-2} y^{-1} and 169 g C m^{-2} y^{-1}. However, prior to soil manipulation, maize showed an average SOC gain of 102 g C m^{-2} y^{-1}.

3.2 Soil resampling method

As a result of soil translocation in 2010, initially measured SOC_{Ap} stocks increased by an average of 780 g C m^{-2}. However, due to the lower C content of the translocated topsoil material (0.76 %), the SOC_{Ap} content of the measurement site dropped by 10 - 14 % after soil manipulation (Tab. 1). Significant differences (paired *t*-test; t = -2.48, $p < 0.09$), which showed an increase in SOC_{Ap} of up to 11 %, were found between SOC_{Ap} stocks measured in 2010 and 2014. Three out of the four chamber positions showed a C gain during the 4 measurement years following soil manipulation. C gains were similar for the upper and lower chamber positions, but lower for the upper middle position. No change in SOC was obtained in the case of the lower middle (Fig. 5; Fig. 6) chamber position.

3.3 Method comparison

Average annual ΔSOC and NECB values for the soil resampling and C budget method, respectively, are shown in Fig. 6. ΔSOC and NECB showed a good overall agreement, with similar tendencies and magnitudes (Fig. 6). Irrespective of the applied method, significant differences were found between SOC stocks measured directly after soil manipulation in 2010 and SOC stocks measured in 2014. Following soil manipulation, both methods revealed similar tendencies in site and chamber-specific changes in SOC (Fig. 6). Both methods indicated a clear C gain for three out of the four chamber positions. C gains derived by the C budget method were similar for the upper, upper middle and lower chamber positions. By contrast, C gains derived by the soil resampling method were slightly but not significantly lower (paired *t*-test; t = -1.23, $p > 0.30$). This was most pronounced for the upper middle chamber position. No change in SOC and only a minor gain in C was observed for the lower middle chamber position according to both methods. Differences between chamber positions indicate the presence of small-scale spatial ΔSOC dynamics typical of soils.

4. Discussion

4.1 Accuracy and precision of applied methods

Despite the similar magnitude and tendencies of the observed NECB and ΔSOC values, both methods were subject to numerous sources of uncertainty, representing the different concepts they are based on (see introduction). These errors affect the accuracy and precision of observed NECB and ΔSOC values differently, which might help to explain differences between the soil resampling and the C budget method.

The soil resampling method is characterized by high measurement precision, which allows for the detection of relatively small changes in SOC. Related uncertainty in derived spatial and temporal ΔSOC dynamics is therefore mainly attributed to the measurement accuracy, affected by sampling strategy and design (Batjes and van Wesemael, 2015; De Gruijter et al., 2006). This includes (i) the spatial distribution of collected samples, (ii) the sampling frequency, (iii) the sampling depth and (iv) whether different components of soil organic matter (SOM) are excluded prior to analyses. The first aspect determines the capability to detect the inherent spatial differences in SOC stocks. This allows the conclusion that point measurements do not necessarily represent AC measurements, which integrate over the spatial variability within their basal area. The second aspect defines the temporal resolution, even though the soil resampling method is not able to perfectly separate spatial from temporal variability because repeated soil samples are biased by inherent spatial variability of the measurement site. The third aspect sets the vertical system boundary, which is often limited because only topsoil horizons are sampled within a number of soil monitoring networks (Van Wesemael et al., 2011) and repeated soil inventories (Leifeld et al., 2011). Similarly, the fourth aspect defines which components of SOM are specifically analyzed.

Usually, coarse organic material is discarded prior to analysis (Schlichting et al., 1995) and therefore, total SOC is not assessed (e.g., roots, harvest residues, etc.).

In comparison, the C budget method considers any type of organic material present in soil by integrating over the total soil depth. As a result, both methods have a different validity range and area, which makes direct quantitative comparison more difficult. This may explain the higher uptake reported for three out of four chamber positions in the case of the C budget method.

In contrast to the soil resampling method, we postulate a higher accuracy and a lower precision in the case of the AC-based C budget method. The reasons for this include a number of potential errors affecting especially the measurement precision of the AC system, whereas over a constant area and maximum soil depth, integrated AC measurements increase measurement accuracy. First, it is currently not clear whether microclimatological and ecophysiological disturbances due to chamber deployment, such as the alteration of temperature, humidity, pressure, radiation, and gas concentration, may result in biased C flux rate estimates (Juszczak et al., 2013; Kutzbach et al., 2007; Lai et al., 2012; Langensiepen et al., 2012). Second, uncertainties related to performed flux separation and gap-filling procedures may influence the obtained annual gaseous C exchange (Gomez-Casanovas et al., 2013; Görres et al., 2014; Moffat et al., 2007; Reichstein et al., 2005). Although continuous operation of the AC system should allow for direct derivation of C budgets from measured CO_2 exchange and annual yields, in practice, data gaps always occur. To fill the measurement gaps, temperature- and PAR-dependent models are derived and used to calculate R_{eco} and GPP, respectively (Hoffmann et al. 2015). Due to the transparent chambers used, modeled R_{eco} is solely based on nighttime measurements. Hence, systematic differences between nighttime and daytime R_{eco} will yield an over- or underestimation of modeled R_{eco}. Because modeled R_{eco} is used to calculate GPP fluxes, GPP will be affected in a similar manner. However, the systematic over- or underestimation of fluxes in both directions may counterbalance the computed NEE, and

455 estimated C budgets may be unaffected. Third, the development of NPP_{shoot} underneath the
456 chamber might be influenced by the permanently installed AC system. Fourth, several minor
457 components such as leaching losses of dissolved inorganic and organic carbon (DIC and DOC), C
458 transport via runoff and atmospheric C deposition were not considered within the applied budgeting
459 approach (see also 2.7).
460 Despite the uncertainties mentioned above, error estimates for annual NEE in this study are within
461 the range of errors presented for annual NEE estimates derived from EC measurements (30 to 50
462 g C m^{-2} y^{-1}) (e.g., Baldocchi, 2003; Dobermann et al., 2006; Hollinger et al., 2005) and below the
463 minimum detectable difference (MDD) reported for most repeated soil inventories (e.g., Batjes and
464 Van Wesemael, 2015; Knebl et al., 2015; Necpálová et al., 2014; Saby et al., 2008; Schrumpf et
465 al., 2011; VandenBygaart, 2006).
466

467 **4.2 Plausibility of observed ΔSOC**

468 Both the soil resampling and the C budget method showed C gains during the four years following
469 soil manipulation. A number of authors calculated additional C sequestration due to soil erosion
470 (Berhe et al., 2007; Dymond, 2010; VandenBygaart et al., 2015; Yoo et al., 2005), which was
471 explained by the burial of replaced C at depositional sites and dynamic replacement at eroded sites
472 (e.g., Doetterl et al., 2016). This is in accordance with erosion-induced C sequestration postulated
473 by, e.g., Berhe and Kleber (2013) and Van Oost et al. (2007). In addition, observed C sequestration
474 could also be a result of the manipulation-induced saturation deficit in SOC. By adding topsoil
475 material from an eroded unsaturated hill slope soil, the capacity and efficiency to sequester C was
476 theoretically increased (Stewart et al., 2007). Hence, additional C was stored at the measurement
477 site. This might be due to physicochemical processes, such as physical protection in macro- and

478 micro aggregates (Six et al., 2002) or chemical stabilization by clay and iron minerals (Kleber et
479 al., 2015).
480 Irrespective of the similar C gain observed by both methods, crop-dependent differences in NECB
481 and thus ΔSOC were only revealed by the C budget method. The reason is the higher temporal
482 resolution of AC-derived C budgets, displaying daily C losses and gains. Observed crop-dependent
483 differences in NECB are in accordance with, e.g., Kutsch et al. (2010), Jans et al. (2010), Hollinger
484 et al. (2005) and Verma et al. (2005), who reported comparable EC-derived C balances for inter
485 alia, maize, sorghum and alfalfa.
486 In 2012, substantial positive annual NECB values were observed. Due to low precipitation during
487 May and June, germination and plant growth of sorghum-Sudan grass was delayed (Fig. 4). As a
488 result, the reproductive phenological stage was drastically shortened. This reduced C losses prior
489 to harvest due to higher R_{eco}:GPP ratios (Wagle et al., 2015). In addition, the presence of cover
490 crops during spring and autumn could have increased SOC, as reported by Lal et al. (2004),
491 Ghimire et al. (2014) and Sainju et al. (2002). No additional C sequestration was observed for
492 alfalfa in 2013 and 2014 or for the lower middle chamber position, which acted neither as a net C
493 source nor sink (Tab. 1; Fig. 5). This opposes the assumption of increased C sequestration by
494 perennial grasses (Paustian et al., 1997) or perennial crops (Zan et al., 2001). However, NEE
495 estimates of alfalfa were within the range of -100 to -400 g C m^{-2}, which is typical for forage crops
496 (*Lolium*, alfalfa, etc.) in different agro-ecosystems (Bolinder et al., 2012; Byrne et al., 2005;
497 Gilmanov et al., 2013; Zan et al., 2001). In addition, Alberti et al. (2010) reported a soil C loss of
498 > 170 g C m^{-2} after crop conversion from continuous maize to alfalfa, concluding that no effective
499 C sequestration occurs in the short-term.

Regardless of the crop type, the AC-derived dynamic NECB values showed that up to 79 % of the standard deviation of estimated annual NECB occurred during the growing season and the main plant growth period from the beginning of July to the end of September.

5. Conclusions

We confirmed that AC-based C budgets are in principle able to detect small-scale spatial differences in NECB and might be thus used to detect spatial heterogeneity of ΔSOC similar to the soil resampling method. However, compared to soil resampling, AC-based C budgets also reveal short-term temporal dynamics (Fig. 5). In addition, AC-based NECB values corresponded well with tendencies and magnitude of ΔSOC values observed by the repeated soil inventory. The period of maximum plant growth was identified as being most important for the development of spatial differences in annual NECB. For upscaling purposes of the presented results, further environmental drivers, processes and mechanisms determining C allocation in space and time within the plant-soil system need to be identified. This type of an approach will be pursued in future within the CarboZALF experimental setup (Sommer et al., 2016; Wehrhan et al., 2016). Moreover, the AC-based C budget method opens new prospects for clarifying unanswered questions, such as the influence of plant development or erosion on NECB and thereon based estimates of ΔSOC.

Acknowledgments

This work was supported by the Brandenburg Ministry of Infrastructure and Agriculture (MIL), who financed the land purchase, the Federal Agency for Renewable Resources (FNR), who co-financed the AC system, and the interdisciplinary research project CarboZALF. The authors want to express their special thanks to Mr. Peter Rakowski for excellent operational and technical

maintenance during the study period as well as to the employees of the ZALF research station, Dedelow, for establishing and maintaining the CarboZALF-D field trial.

References

Alberti, G., Delle Vedove, G.D., Zuliani, M., Peressotti, A., Castaldi, S., Zerbi, G., 2010. Changes in CO_2 emissions after crop conversion from continuous maize to alfalfa. Agric. Ecosyst. Environ. 136, 139-147.

Baldocchi, D.D., 2003. Assessing the eddy covariance technique for evaluating carbon dioxide exchange rates of ecosystems: past, present and future. Glob. Change Biol. 9, 479-492.

Batjes, N.H., van Wesemael, B., 2015. Measuring and monitoring soil carbon, in: Banwart, S. A., Noellemeyer, E., Milne, E. (Eds.), Soil Carbon: Science, Management and Policy for Multiple Benefits. SCOPE Series 71. CABI, Wallingford, UK, pp. 188-201.

Berhe, A.A., Harte, J., Harden, J.W., Torn, M.S., 2007. The significance of the erosion-induced terrestrial carbon sink. BioScience 57, 337-346.

Berhe, A.A., Kleber, M., 2013. Erosion, deposition, and the persistence of soil organic matter: mechanistic consideration and problems with terminology. Earth Surf. Processes Landforms 38, 908-912.

Bolinder, M.A., Kätterer, T., Andrén, O., Parent, L.E., 2012. Estimating carbon inputs to soil in forage-based crop rotations and modeling the effects on soil carbon dynamics in a Swedish long-term field experiment. Can. J. Soil. Sci. 92, 821-833.

Byrne, K.A., Kiely, G., Leahy, P., 2005. CO_2 fluxes in adjacent new and permanent temperate grasslands. Agric. For. Meteorol. 135, 82–92.

545 Chen, L., Smith, P., Yang, Y., 2015. How has soil carbon stock changed over recent decades? Glob.
546 Change Biol. 21, 3197-3199.
547 Conant, R.T., Ogle, S.M., Paul, E.A., Paustian, K., 2011. Measuring and monitoring soil organic
548 carbon stocks in agricultural lands for climate mitigation. Front. Ecol. Environ. 9, 169-173.
549 Culman, S.W., Snapp, S.S., Green, J.M., Gentry, L.E., 2013. Short- and long-term labile soil carbon
550 and nitrogen dynamics reflect management and predict corn agronomic performance.
551 Agron. J. 105, 493-502.
552 Davidson, E. A., Savage, K., Verchot, L. V., Navarro, R., 2002. Minimizing artifacts and biases in
553 chamber-based measurements of soil respiration. Agric. For. Meteorol. 113, 21-37.
554 De Gruijter, J.J., Brus, D.J., Bierkens, M.F.P., Knotters, M., 2006. Sampling for Natural Resource
555 Monitoring. Springer Verlag, Berlin.
556 Deumlich, D., Rogasik, H., Hierold, W., Onasch, I., Völker, L., Sommer, M., 2017 (in print). The
557 CarboZALF-D manipulation experiment – experimental design and SOC patterns. Int. j.
558 environ. agric. res. 3, 40-50.
559 Dobermann, A.R., Walters, D.T., Baker, J.M., 2006. Comment on "Carbon budget of mature no-
560 till ecosystem in north central region of the United States." Agric. For. Meteorol. 136, 83-
561 84.
562 Doetterl, S., Berhe, A.A., Nadeu, E., Wang, Z., Sommer, M., Fiener, P., 2016. Erosion, deposition
563 and soil carbon: a review of process-level controls, experimental tools and models to
564 address C cycling in dynamic landscapes. Earth Sci. Rev. 154, 102-122.
565 Dymond, J.R., 2010. Soil erosion in New Zealand is a net sink of CO_2. Earth Surf. Processes
566 Landforms 35, 1763-1772. doi:10.1002/esp.2014.
567 Eickenscheidt, T., Freibauer, A., Heinichen, J., Augustin, J., Drösler, M., 2014. Short-term effects
568 of biogas digestate and cattle slurry application on greenhouse gas emissions affected by N

availability from grasslands on drained fen peatlands and associated organic soils. Biogeosciences 11, 6187-6207.

Elsgaard, L., Görres, C., Hoffmann, C.C., Blicher-Mathiesen, G., Schelde, K., Petersen, S.O., 2012. Net ecosystem exchange of CO_2 and carbon balance for eight temperate organic soils under agricultural management. Agric. Ecosyst. Environ. 162, 52-67.

Foken, T., 2008. Micrometeorology. Springer Verlag, Berlin.

Ghimire, R., Norton, J.B., Pendall, E., 2014. Alfalfa-grass biomass, soil organic carbon, and total nitrogen under different management approaches in an irrigated agroecosystem. Plant Soil 374, 173-184.

Gilmanov, T.G., Soussana, J.F., Aires, L., Allard, V., Ammann, C., Balzarolo, M., Barcza, Z., Bernhofer, C., Campbell, C.L., Cernusca, A., Cescatti, A., Clifton-Brown, J., Dirks, B.O.M., Dore, S., Eugster, W., Fuhrer, J., Gimeno, C., Gruenwald, T., Haszpra, L., Hensen, A., Ibrom, A., Jacobs, A.F.G., Jones, M.B., Lanigan, G., Laurila, T., Lohila, A., Manca, G., Marcolla, B., Nagy, Z., Pilegaard, K., Pinter, K., Pio, C., Raschi, A., Rogiers, N., Sanz, M.J., Stefani, P., Sutton, M., Tuba, Z., Valentini, R., Williams, M.L., Wohlfahrt, G., 2007. Partitioning European grassland net ecosystem CO_2 exchange into gross primary productivity and ecosystem respiration using light response function analysis. Agric. Ecosyst. Environ. 121, 93–120.

Gilmanov, T.G., Wylie, B.K., Tieszen, L.L., Meyers, T.P., Baron, V.S., Bernacchi, C.J., Billesbach, D.P., Burba, G.G., Fischer, M.L., Glenn, A.J., Hanan, N.P., Hatfield, J.L., Heuer, M.W., Hollinger, S.E., Howard, D.M., Matamala, R., Prueger, J.H., Tenuta, M., Young, D.G., 2013. CO_2 uptake and ecophysiological parameters of the grain crops of midcontinent North America: estimates from flux tower measurements. Agric. Ecosyst. Environ. 164, 162–175.

593 Gomez-Casanovas, N., Anderson-Teixeira, K., Zeri, M., Bernacchi, C.J., DeLucia, E.H., 2013. Gap
594 filling strategies and error in estimating annual soil respiration. Glob. Change Biol. 19,
595 1941-1952.
596 Görres, C.-M., Kutzbach, L., Elsgaard, L., 2014. Comparative modeling of annual CO_2 flux of
597 temperate peat soils under permanent grassland management. Agric. Ecosyst. Environ. 186,
598 64–76.
599 Hernandez-Ramirez, G., Hatfield, J.L., Parkin, T.B., Sauer, T.J., Prueger, J.H., 2011. Carbon
600 dioxide fluxes in corn-soybean rotation in the midwestern U.S.: inter- and intra-annual
601 variations, and biophysical controls. Agric. For. Meteorol. 151, 1831-1842.
602 Hoffmann, M., Jurisch, N., Borraz, E.A., Hagemann, U., Drösler, M., Sommer, M., Augustin, J.,
603 2015. Automated modeling of ecosystem CO_2 fluxes based on periodic closed chamber
604 measurements: a standardized conceptual and practical approach. Agric. For. Meteorol.
605 200, 30-45.
606 Hollinger, S.E., Bernacchi, C.J., Meyers, T.P., 2005. Carbon budget of mature no-till ecosystem in
607 north central region of the United States. Agric. For. Meteorol. 130, 59-69.
608 IUSS Working Group WRB, 2015. World reference base for soil resources 2014. International soil
609 classification system for naming soils and creating legends for soil maps. Update 2015.
610 World Soil Resources Reports No. 106. FAO, Rome.
611 Jans, W.W.P., Jacobs, C.M.J., Kruijt, B., Elbers, J.A., Barendse, S., Moors, E.J., 2010. Carbon
612 exchange of a maize (*Zea mays* L.) crop: influence of phenology. Agric. Ecosyst. Environ.
613 139, 316-324.
614 Juszczak, R., Humphreys, E., Acosta, M., Michalak-Galczewska, M., Kayzer, D., Olejnik, J., 2013.
615 Ecosystem respiration in a heterogeneous temperate peatland and its sensitivity to peat
616 temperature and water table depth. Plant Soil 366, 505-520.

Kleber, M., Eusterhues, K., Keiluweit, M., Mikutta, C., Mikutta, R., Nico, P. S., 2015. Chapter one – Mineral-Organic associations: Formation, Properties, and relevance in soil environments. Adv. Agro. 130, 1-140.

Knebl, L., Leithold, G., Brock, C., 2015. Improving minimum detectable differences in the assessment of soil organic matter change in short-term field experiments. J. Plant Nutr. Soil Sci. 178, 35-42.

Koskinen, M., Minkkinen, K., Ojanen, P., Kämäräinen, M., Laurila, T., Lohila, A., 2014. Measurements of CO_2 exchange with an automated chamber system throughout the year: challenges in measuring night-time respiration on porous peat soil. Biogeosciences 11, 347-363.

Kutsch, W.L., Aubinet, M., Buchmann, N., Smith, P., Osborne, B., Eugster, W., Wattenbach, M., Schrumpf, M., Schulze, E.D., Tomelleri, E., Ceschia, E., Bernhofer, C., Béziat, P., Carrara, A., Di Tommasi, P., Grünwald, T., Jones, M., Magliulo, V., Marloie, O., Moureaux, C., Olioso, A., Sanz, M.J., Saunders, M., Søgaard, H., Ziegler, W., 2010. The net biome production of full crop rotations in Europe. Agric. Ecosyst. Environ. 139, 336-345.

Kutzbach, L., Schneider, J., Sachs, T., Giebels, M., Nykänen, H., Shurpali, N.J., Martikainen, P.J., Alm, J., Wilmking, M., 2007. CO_2 flux determination by closed-chamber methods can be seriously biased by inappropriate application of linear regression. Biogeosciences 4, 1005-1025.

Lai, D.Y.F., Roulet, N.T., Humphreys, E.R., Moore, T.R., Dalva, M., 2012. The effect of atmospheric turbulence and chamber deployment period on autochamber CO_2 and CH_4 flux measurements in an ombrotrophic peatland. Biogeosciences 9, 3305-3322.

Lal, R., Griffin, M., Apt, J., Lave, L., Morgan, G., M., 2004. Managing Soil carbon. Science 304, 393.

641 Langensiepen, M., Kupisch, M., van Wijk, M.T., Ewert, F., 2012. Analyzing transient closed
642 chamber effects on canopy gas exchange for flux calculation timing. Agric. For. Meteorol.
643 164, 61-70.
644 Leiber-Sauheitl, K., Fuß, R., Voigt, C., Freibauer, A., 2013. High greenhouse gas fluxes from
645 grassland on histic gleysol along soil C and drainage grasslands. Biogeosciences. 11, 749-
646 761.
647 Leifeld, J., Ammann, C., Neftel, A., Fuhrer, J., 2011. A comparison of repeated soil inventory and
648 carbon flux budget to detect soil carbon stock changes after conversion from cropland to
649 grasslands. Glob. Change Biol. 17, 3366-3375.
650 Leifeld, J., Bader, C., Borraz, E., Hoffmann, M., Giebels, M., Sommer, M., Augustin, J., 2014. Are
651 C-loss rates from drained peatlands constant over time? The additive value of soil profile
652 based and flux budget approach. Biogeosci. Discuss. 11, 12341-12373.
653 Livingston, G.P., Hutchinson, G.L., 1995. Enclosure-based measurement of trace gas exchange:
654 applications and sources of error, in: Matson, P.A., Harris, R.C. (Eds.), Methods in Ecology.
655 Biogenic Trace Gases: Measuring Emissions from Soil and Water. Blackwell Science,
656 Oxford, UK, pp. 14–51.
657 Lloyd, J., Taylor, J.A., 1994. On the temperature dependence of soil respiration. Funct. Ecol. 8,
658 315-323.
659 Luo, Y., Ahlström, A., Allison, S.D., Batjes, N.H., Brovkin, V., Carvalhais, N., Chappell, A., Ciais,
660 P., Davidson, E.A., Finzi, A., Georgiou, K., Guenet, B., Hararuk, O., Harden, J.W., He, Y.,
661 Hopkins, F., Jiang, L., Koven, C., Jackson, R.B., Jones, C.D., Lara, M.J., Liang, J.,
662 McGuire, A.D., Parton, W., Peng, C., Randerson, J.T., Salazar, A., Sierra, C.A., Smith,
663 M.J., Tian, H., Todd-Brown, K.E.O., Torn, M., van Groenigen, k.J., Wang, Y.P., West, t.o.,
664 Wie, Y., Wieder, W.R., Xia, J., Xu, X., Xu, X., Zhou, T., 2016. Toward more realistic

projections of soil carbon dynamics by Earth system models. Global Biogeochem. Cycles 30, 40-56.

Moffat, A.M., Papale D., Reichstein M., Hollinger, D.Y., Richardson, A.D., Barr, A.G., Beckstein, C., Braswell, B.H., Churkina, G., Desai, A.R., Falge, E., Gove, J.H., Heimann, M., Hui, D., Jarvis, A.J., Kattge, J., Noormets, A., Stauch, V.J., 2007. Comprehensive comparison of gap-filling techniques for eddy covariance net carbon fluxes. Agric. For. Meteorol. 147, 209–232.

Necpálová, M., Anex Jr., R.P., Kravchenko, A.N., Abendroth, L.J., Del Grosso, S.J., Dick, W.A., Helmers, M.J., Herzmann, D., Lauer, J.G., Nafziger, E.D., Sawyer, J.E., Scharf, P.C., Strock, J.S., Villamil, M.B., 2014. What does it take to detect a change in soil carbon stock? A regional comparison of minimum detectable difference and experiment duration in the north central United States. J. Soils Water Conserv. 69, 517-531.

Paustian, K., Collins, H.P., Paul, E.A., 1997. Management controls on soil carbon, in: Paul, E.A., Paustian, K., Elliott, E.T., Cole, C.V. (Eds.), Soil Organic Matter in Temperate Agroecosystems: Long-Term Experiments in North America. CRC Press, Boca Raton, FL, pp. 15-50.

Poeplau, C., Bolinder, M.A., Kätterer, T., 2016. Towards an unbiased method for quantifying treatment effects on soil carbon in long-term experiments considering initial within-field variation. Geoderma 267, 41-47.

Pohl, M., Hoffmann, M., Hagemann, U., Giebels, M., Albiac Borraz, E., Sommer, M., Augustin, J., 2014. Dynamic C and N stocks–key factors controlling the C gas exchange of maize in a heterogeneous peatland. Biogeosciences 11, 2737-2752.

Reichstein, M., Falge, E., Baldocchi, D., Papale, D., Aubinet, M., Berbiger, P., Bernhofer, C., Buchmann, N., Gilmanov, T., Granier, A., Grünwald, T., Havránková, K., Ilvesniemi, H.,

689 Janous, D., Knohl, A., Laurila, T., Lohila, A., Loustau, D., Metteucci, G., Meyers, T.,
690 Miglietta, F., Ourcival, J.-M., Pumpanen, J., Rambal, S., Rotenberg, E., Sanz, M.,
691 Tenhunen, J., Seufert, G., Vaccari, F., Vesala, T., Yakir, D., Valentini, R., 2005. On the
692 separation of net ecosystem exchange into assimilation and ecosystem respiration: review
693 and improved algorithm. Global Change Biol. 11, 1424–1439.
694 Rieckh, H., Gerke, H.H., Sommer, M., 2012. Hydraulic properties of characteristic horizons
695 depending on relief position and structure in a hummocky glacial soil landscape. Soil
696 Tillage Res. 125, 123-131.
697 Saby, N.P.A., Bellamy, P.H., Morvan, X., Arrouays, D., Jones, R.J.A., Verheijen, F.G.A.,
698 Kibblewhite, M.G., Verdoodt, A., Üveges, J.B., Freudenschuß, A., Simota, C., 2008. Will
699 European soil-monitoring networks be able to detect changes in topsoil organic carbon
700 content? Glob. Change Biol. 14, 2432-2442.
701 Sainju, U.M., Singh, B.P., Whitehead, W.F., 2002. Long-term effects of tillage, cover crops, and
702 nitrogen fertilization on organic carbon and nitrogen concentrations in sandy loam soils in
703 Georgia, USA. Soil Tillage Res. 63, 167-179.
704 Savage, K.E., Davidson, E.A., 2003. A comparison of manual and automated systems for soil CO_2
705 flux measurements: trade-offs between spatial and temporal resolution. J. Exp. Bot. 54,
706 891-899.
707 Schlichting, E., Blume, H.P., Stahr, K., Soils Practical (in German). Blackwell, Berlin, 1995.
708 Schrumpf, M., Schulze, E. D., Kaiser, K., Schumacher, J., 2011. How accurately can soil organic
709 carbon stocks and stock changes be quantified by soil inventories? Biogeosciences 8, 1193-
710 1212.
711 Six, J., Conant, R.T., Paul, E.A., Paustian, K., 2002. Stabilization mechanisms of soil organic
712 matter: implications for C-saturation of soils. Plant Soil 241, 155-176.

713 Skinner, R.H., Dell, C.J., 2015. Comparing pasture C sequestration estimates from eddy covariance
714 and soil cores. Agric. Ecosyst. Eviron. 199, 52-57.
715 Smith, P., Lanigan, G., Kutsch, W. L., Buchmann, N., Eugster, W., Aubinet, M., Ceschia, E.,
716 Béziat, P., Yeluripati, J. B., Osborne, B., Moors, E. J., Brut, A., Wattenbach, M., Saunders,
717 M., Jones, M., 2010. Measurements necessary for assessing the net ecosystem carbon
718 budget of croplands. Agric. Ecosyst. Eviron. 139, 302-315.
719 Sommer, M., Augustin, J., Kleber, M., 2016. Feedbacks of soil erosion on SOC patterns and carbon
720 dynamics in agricultural landscapes – the CarboZALF experiment. Soil Tillage Res. 156,
721 182-184.
722 Stewart, C.E., Paustian, K., Conant, R.T., Plante, A.F., Six, J., 2007. Soil carbon saturation:
723 concept, evidence and evaluation. Biogeochemistry 86, 19-31.
724 Stockmann, U., Padarian, J., McBratney, A., Minasny, B., de Brogniez, D., Montanarella, L., Hong,
725 Y., S., Rawlins, B.G., Filed, D.J., 2015. Global soil organic carbon assessment. Glob. Food
726 Secur. 6, 9-16.
727 Van Oost, K., Quine, T.A., Govers, G., De Gryze, S., Six, J., Harden, J.W., Ritchie, J.C., McCarty,
728 G.W., Heckrath, G., Kosmas, C., Giraldez, J.V., da Silva, J.R., Merckx, R., 2007. The
729 impact of agricultural soil erosion on the global carbon cycle. Science 318, 626-629.
730 Van Wesemael, B., Paustian, K., Andrén, O., Cerri, C.E.P., Dodd, M., Etchevers, J., Goidts, E.,
731 Grace, P., Kätterer, T., McConkey, B.G., Ogle, S., Pan, G., Siebner, C., 2011. How can soil
732 monitoring networks be used to improve predictions of organic carbon pool dynamics and
733 CO_2 fluxes in agricultural soils? Plant Soil 338, 247-259.
734 VandenBygaart, A.J., 2006. Monitoring soil organic carbon stock changes in agricultural
735 landscapes: issues and a proposed approach. Can. J. Soil Sci. 86, 451-463.

VandenBygaart, A.J., Gregorich, E.G., Helgason, B.L., 2015. Cropland C erosion and burial: is buried soil organic matter biodegradable? Geoderma 239-240, 240-249.

Verma, S.B., Dobermann, A., Cassman, K.G., Walters, D.T., Knops, J.M., Arkebauer, T.J., Suyker, A.E., Burba, G.G., Amos, B., Yang, H., Ginting, D., Hubbard, K.G., Gitelson, A.A., Walter-Shea, E.A., 2005. Annual carbon dioxide exchange in irrigated and rainfed maize-based agroecosystems. Agric. For. Meteorol. 131, 77-96.

Wagle, P., Kakani, V.G., Huhnke, R.L., 2015. Net ecosystem carbon dioxide exchange of dedicated bioenergy feedstocks: switchgrass and high biomass sorghum. Agric. For. Meteorol. 207, 107-116.

Wang, K., Liu, C., Zheng, X., Pihlatie, M., Li, B., Haapanala, S., Vesala, T., Liu, H., Wang, Y., Liu, G., Hu, F., 2013. Comparison between eddy covariance and automatic chamber techniques for measuring net ecosystem exchange of carbon dioxide in cotton and wheat fields. Biogeosciences 10, 6865-6877.

Wehrhan, M., Rauneker, P., Sommer, M., 2016. UAV-based estimation of carbon exports from heterogeneous soil landscapes - a case study from the CarboZALF experimental area. Sensors (Basel) 16, 255.

Wuest, S., 2014. Seasonal variation in soil organic carbon. Soil Sci. Soc. Am. J. 78, 1442-1447.

Xiong, X., Grunwald, S., Corstanje, R., Yu, C., Bliznyuk, N., 2016. Scale-dependent variability of soil organic carbon coupled to land use and land cover. Soil Tillage Res. 160, 101-109.

Yin, X., Goudriaan, J., Lantinga, E.A., Vos, J., Spiertz, H.J., 2003. A flexible sigmoid function of determinate growth. Ann. Bot. 91, 361-371.

Yoo, K., Amundson, R., Heimsath, A.M., Dietrich, W.E., 2005. Erosion of upland hillslope soil organic carbon: coupling field measurements with a sediment transport model. Global Biogeochem. Cycles 19, 1-17.

760 Zan, C.S., Fyles, J.W., Girouard, P., Samson, R.A., 2001. Carbon sequestration in perennial
761 bioenergy, annual corn and uncultivated systems in southern Quebec. Agric. Ecosyst.
762 Environ. 86, 135-144.
763 Zeide, B., 1993. Analysis of growth equations. For. Sci. 39, 594-616.
764

765 **List of tables:**

766 **Tab. 1.:** Chamber-specific annual sums of CO_2 exchange (R_{eco}, GPP, NEE), NPP_{shoot}, NECB and
767 ΔSOC (± uncertainty), as well as corresponding environmental variables measured during the study
768 period from 2010 to 2014.

769 **A.1.:** Management information regarding the study period from 2010 to 2014. Gray shaded rows
770 indicate coverage by chamber measurements.

771

772 **List of figures:**

773 **Fig. 1.:** Schematic representation of the study concept used to detect changes in soil organic carbon
774 stock (ΔSOC). Black stars represent SOC measured by the soil resampling method. Black circles
775 represent annual NECB derived using the C budget method.

776 **Fig. 2.:** Transect of automatic chambers and chamber positions within the depression overlying the
777 Endogleyic Colluvic Regosol (WRB 2015, left). The black arrow shows the position of the
778 datalogger and controlling devices, which were placed within a wooden, weather-sheltered house.
779 The soil profile is shown on the right. Soil horizon-specific SOC (%) and Nt (%) contents are
780 indicated by solid and dashed vertical white lines, respectively. Spatial differences in NECB and
781 the basic principle of the C budget method are shown as the scheme within the picture.

Fig. 3.: Time series of CO_2 exchange (A-D) for the four chambers of the AC system during the study period from 2010 to 2014. R_{eco} (black), GPP (light gray) and NEE (dark gray) are shown as daily sums (y-axis). NEE_{cum} is presented as a solid line, representing the sum of continuously accumulated daily NEE values (secondary y-axis). The presented values display cumulative NEE following soil manipulation to the end of 2014. Note the different scales of the y-axes. The grey shaded area represents the period prior to soil manipulation. The dashed vertical line indicates the soil manipulation. Dotted lines represent harvest events.

Fig. 4.: Time series of modeled aboveground biomass development (NPP_{shoot}) (A-D) for the four chambers of the AC system during the study period from 2010 to 2014. NPP_{shoot} is shown as cumulative values. The presented values display cumulative NPP_{shoot} following soil manipulation to the end of 2014. The biomass model is based on biomass sampling (2010-2012) and biweekly LAI measurements (2013-2014) during crop growth (grey dots). C removal due to chamber harvests is shown by black dots. The grey shaded area represents the period prior to soil manipulation. The dashed vertical line indicates the soil manipulation. Dotted lines represent harvest events.

Fig. 5.: Temporal and spatial dynamics in cumulative NECB and ΔSOC throughout the study period based on (A) the C budget method (measured/modeled; black lines) and (B) the soil resampling method (linear interpolation; gray lines), respectively. The grey shaded area represents the period prior to soil manipulation. The dashed vertical line indicates the soil manipulation. Dotted lines represent harvest events. Temporal dynamics in NECB revealed by the C budget method allow for the identification of periods being most important for changes in SOC. Major spatial deviation occurred during the maximum plant growth period (May to September). The

proportion (%) of these periods with respect to the standard deviation of estimated annual NECB accounted for up to 79 %.

Fig. 6.: Average annual ΔSOC observed after soil manipulation (April 2011 to December 2014) by soil resampling and the C budget method for (A) the entire measurement site and (B) single chamber positions within the measured transect. ΔSOC represents the change in carbon storage, with positive values indicating C sequestration and negative values indicating C losses. Error bars display estimated uncertainty for the C budget method and the analytical error of ± 5 % for the soil resampling method. A perfomed Wilcoxon rank-sum test showed no significant difference between NECB and ΔSOC values obtained by both methodological approaches for all four chambers (p-value=0.25).

A.3.: Time series of recorded environmental conditions throughout the study period from 2010 to 2014. Daily Precipitation and GWL are shown for the upper (solid line) and lower (dashed line) chamber position in the upper panel (A). The lower panel (B) shows the mean daily air temperature. The grey shaded area represents the period prior to soil manipulation. The dashed vertical line indicates the soil manipulation.

823 **Tab.1**

Year	Crop rotation	Position	R_{eco}	GPP	NEE	NECB*	NPP_{shoot}		NPP_{shoot}			SOC to 1 m depth	SOC in Ap horizon	ΔSOC	Nt to 1 m depth	Nt in Ap horizon	Precip.	GWL
							harvested	modeled	N	P	K							
				(g C m^{-2})			(g C m^{-2})			(g m^{-2})		(Kg m^{-2} 1 m^{-1})	(Kg m^{-2} 0.3 m^{-1})	(g C m^{-2})	(Kg m^{-2} 1 m^{-1})	(Kg m^{-2} 0.3 m^{-1})	(mm)	(cm)
2010	maize	A (upper)	1014 ±9	-1845 ±8	-831^{a} ±12	86 ±66	744	745^{a}±65	28.1	5.0	25.6	11.6	5.1		1.3	0.6	516	135
		B (upper middle)	987 ±11	-1970^{a} ±8	-983 ±13	251 ±66	727	732^{a} ±64	24.7	4.1	18.0	9.1	4.2		0.9	0.4		103
		C (lower middle)	1064 ±38	-2000 ^{a} ±11	-935^{a} ±40	190 ±77	744	745^{a} ±65	25.5	4.2	16.9	9.1	4.2	-	0.9	0.4		95
		D (lower)	1110 ±21	-1737 ±10	-627^{a} ±23	-118 ±69	744	745^{a} ±65	25.0	4.2	18.2	12.8	5.0		1.3	0.5		69
2011	maize	A (upper)	891 ±13	-2022 ±18	-1131^{a} ±22	-149 ±103	1238	1280^{a} ±101	29.5	5.4	30.2	10.5	3.5		1.1	0.4	618	129
		B (upper middle)	855^{a} ±10	-1894 ±13	-1039^{a} ±16	-169 ±96	1167	1208^{a} ±95	36.4	5.9	32.7	8.7	3.4		0.9	0.4		97
		C (lower middle)	980 ±14	-2062 ±25	-1082 ±28	-79 ±95	1115	1161^{a} ±91	33.7	5.6	32.9	9.0	3.7		0.9	0.4		87
		D (lower)	843^{a} ±31	-1730 ±8	-888 ±32	-59 ±80	900	947^{a} ±73	35.0	5.7	31.8	12.2	4.0		1.3	0.4		61
2012	winter wheat	A (upper)	1058 ±86	-2659 ±12	-1600 ±87	648 ±104	297**/634	952^{a} ±56	36.3	6.3	42.6						585	139
		B (upper middle)	1075 ±8	-2591 ±11	-1516 ±13	472 ±65	310**/727	1044^{a} ±64	33.3	5.8	37.5							107
		C (lower middle)	1286 ±8	-2617 ±9	-1331 ±12	346 ±60	310**/665	985^{a} ±59	32.7	5.4	35.5		-	-				87
	sorghum	D (lower)	1044 ±10	-2194 ±9	-1150 ±13	430 ±39	299**/420	720^{a} ±37	33.9	5.8	40.4							61
2013		A (upper)	1140 ±83	-1583 ±9	-443 ±83	43 ±91	290	400^{a,b} ±37	14.0	1.7	11.6					-	499	154
		B (upper middle)	1283 ±80	-1819 ±8	-536 ±80	93 ±86	304	443^{b} ±32	14.7	1.8	12.1							122
		C (lower middle)	1438 ±20	-1726 ±7	-288 ±22	-107 ±36	324	395^{a} ±29	15.6	1.9	12.9							94
		D (lower)	1587 ±80	-2036 ±8	-448 ±80	6 ±87	329	442^{b} ±34	15.9	2.0	13.2							68
2014	alfalfa	A (upper)	1161 ±15	-1615 ±7	-455^{a} ±16	-126 ±26	605	581^{a} ±20	29.2	3.6	24.2	10.9	3.9	376	1.2	0.5	591	181
		B (upper middle)	1443 ±18	-2063 ±7	-619^{a} ±19	52 ±28	635	567^{a} ±20	30.7	3.8	25.4	8.9	3.5	156	0.9	0.4		149
		C (lower middle)	1683 ±18	-2111 ±6	-428 ±19	-36 ±26	632	535^{a} ±18	30.5	3.8	25.3	9.0	3.7	0	0.9	0.5		121
		D (lower)	1584 ±12	-2113 ±14	-528 ±19	-52 ±28	587	580^{a} ±21	28.3	3.5	23.5	12.5	4.2	276	1.3	0.4		95
	annual average (2011-2014)	A (upper)	1063 ±49	-1970 ±12	-901 ±52	98 ±43	766	803 ±54	27.3	4.3	27.2			94 ±43				151
		B (upper middle)	1164 ±29	-2092 ±10	-919 ±32	104 ±37	786	815 ±53	28.8	4.3	26.9			39 ±43				119
		C (lower middle)	1347 ±15	-2129 ±12	-779 ±20	10 ±30	762	769 ±49	28.1	4.2	26.7		-	0 ±46		-	573	97
		D (lower)	1265 ±33	-2018 ±10	-739 ±38	67 ±32	634	672 ±41	28.3	4.3	27.2			69 ±47				71
		site	1209 ±32	-2052 ±11	-843 ±36	78 ±18	737	765 ±49	28.1	4.3	27.0			51 ±18				156

824 *for comparability reasons the NECB is given using the soil sign convention (negative values = soil C loss; positive values = soil C gain)

825 **NPP_{shoot} is based on biomass samples collected next to each chamber because no chamber harvest was performed for *winter fodder rye* in 2012; superscript letter indicate non-significant differences

826 (Wilcoxon rank sum test; p-value > 0.05) between measured CO_2 fluxes and NPP_{shoot}.

827 **Fig. 1**

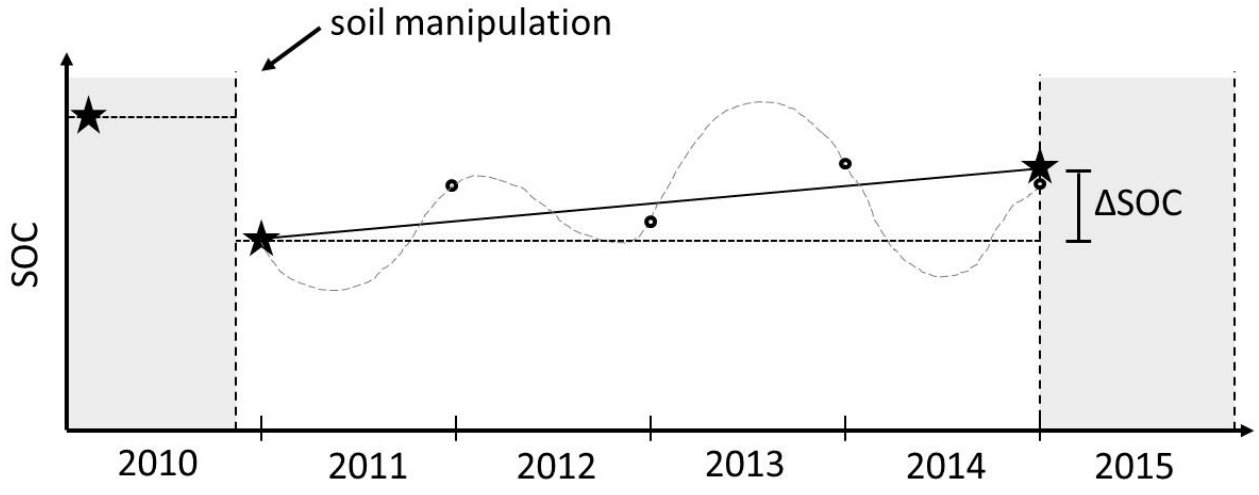

828

829

830

831

832

833

834

835

836

837

838

839

840

841

842 **Fig. 2**

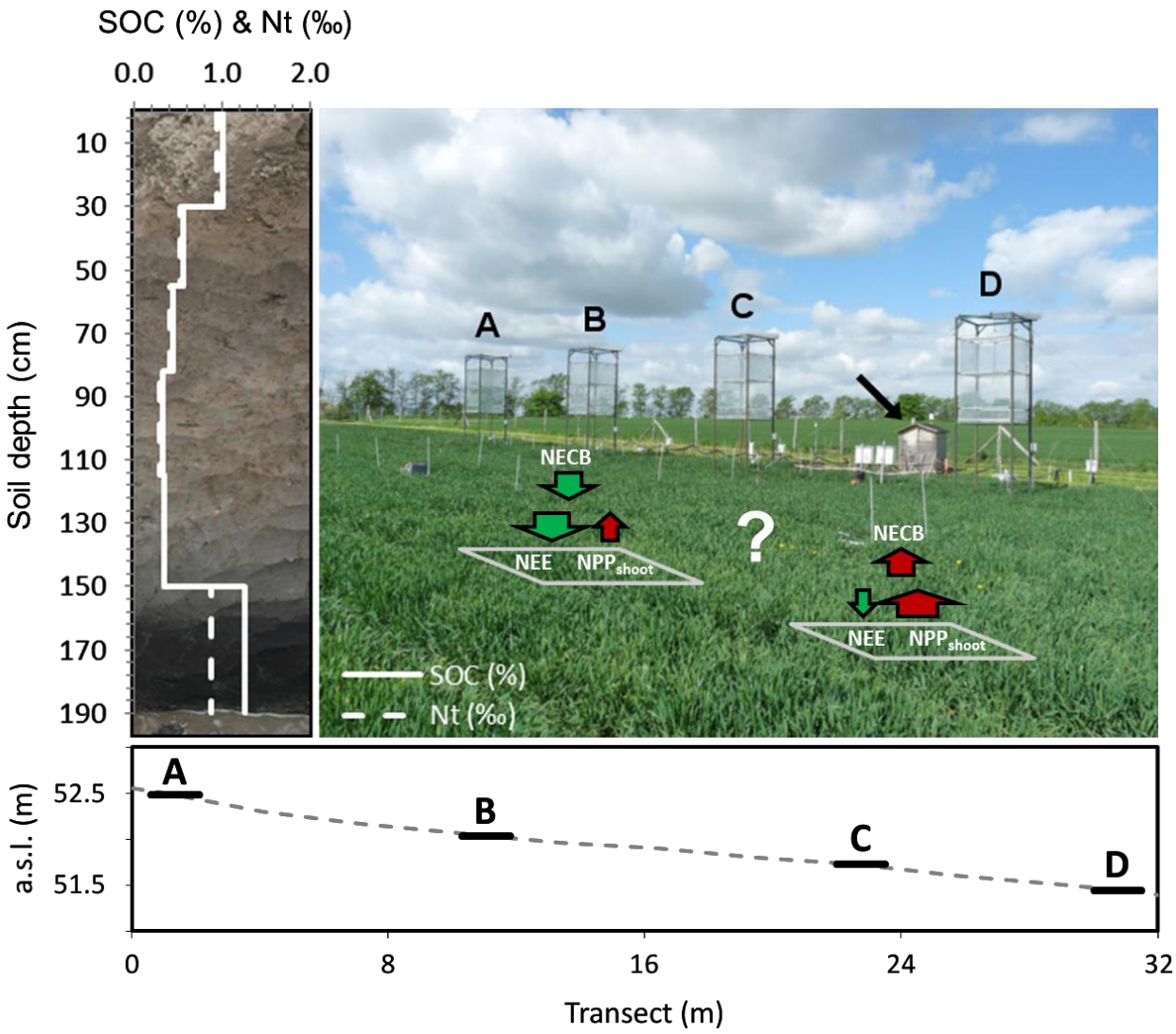

843

844

845

846

847

848

849

Fig. 3

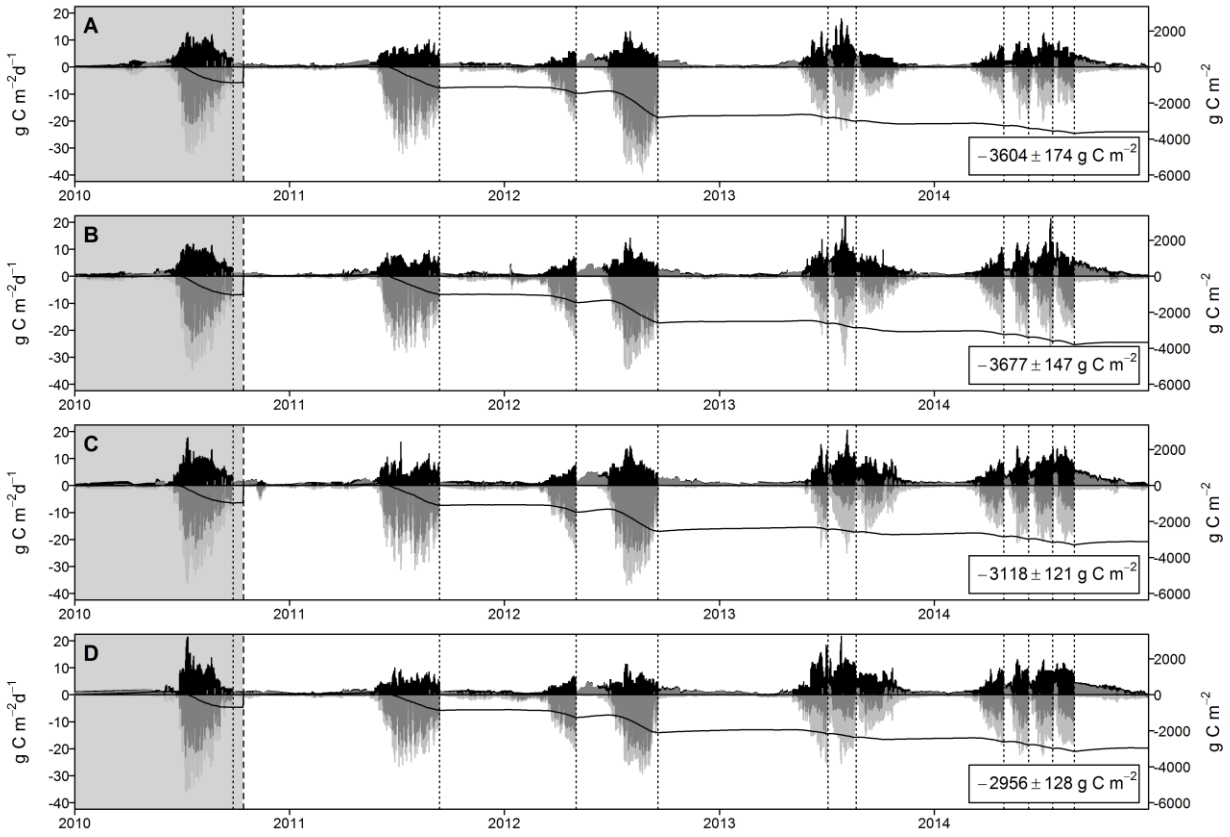
A
B
C
D
g C m^{-2}d^{-1}
g C m^{-2}
−3604 ± 174 g C m^{-2}
−3677 ± 147 g C m^{-2}
−3118 ± 121 g C m^{-2}
−2956 ± 128 g C m^{-2}
2010
2011
2012
2013
2014

Fig. 4

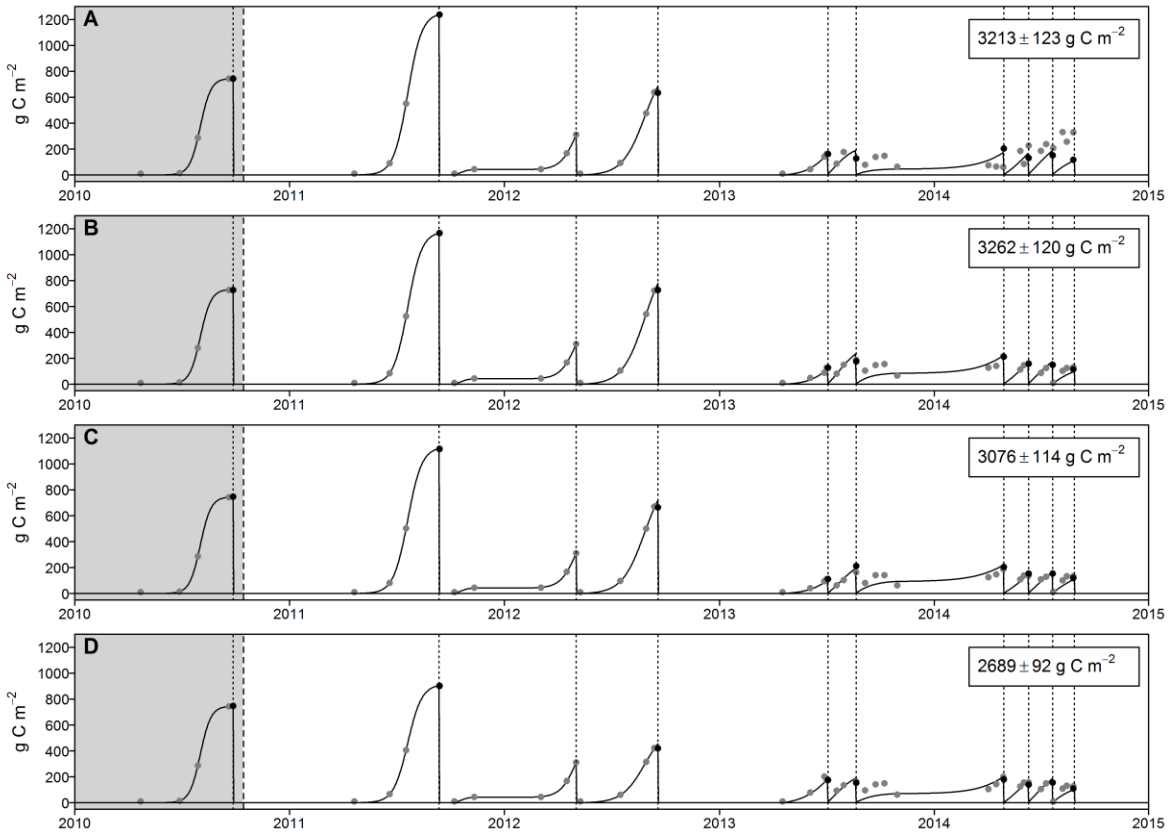
A
3213 ± 123 g C m^{-2}
B
3262 ± 120 g C m^{-2}
C
3076 ± 114 g C m^{-2}
D
2689 ± 92 g C m^{-2}
g C m^{-2}
0
200
400
600
800
1000
1200
2010
2011
2012
2013
2014
2015

872 **Fig. 5**

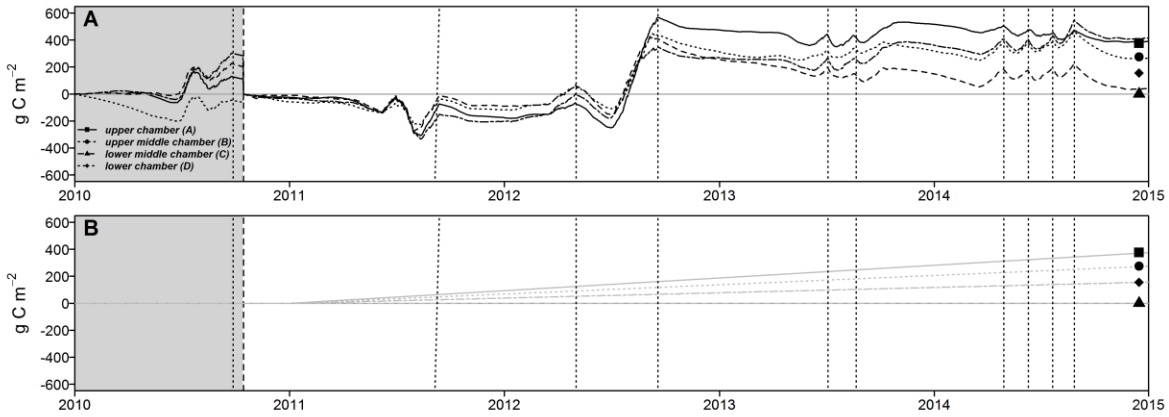

873

874

875

876

877

878

879

880

881

882

883 **Fig. 6**

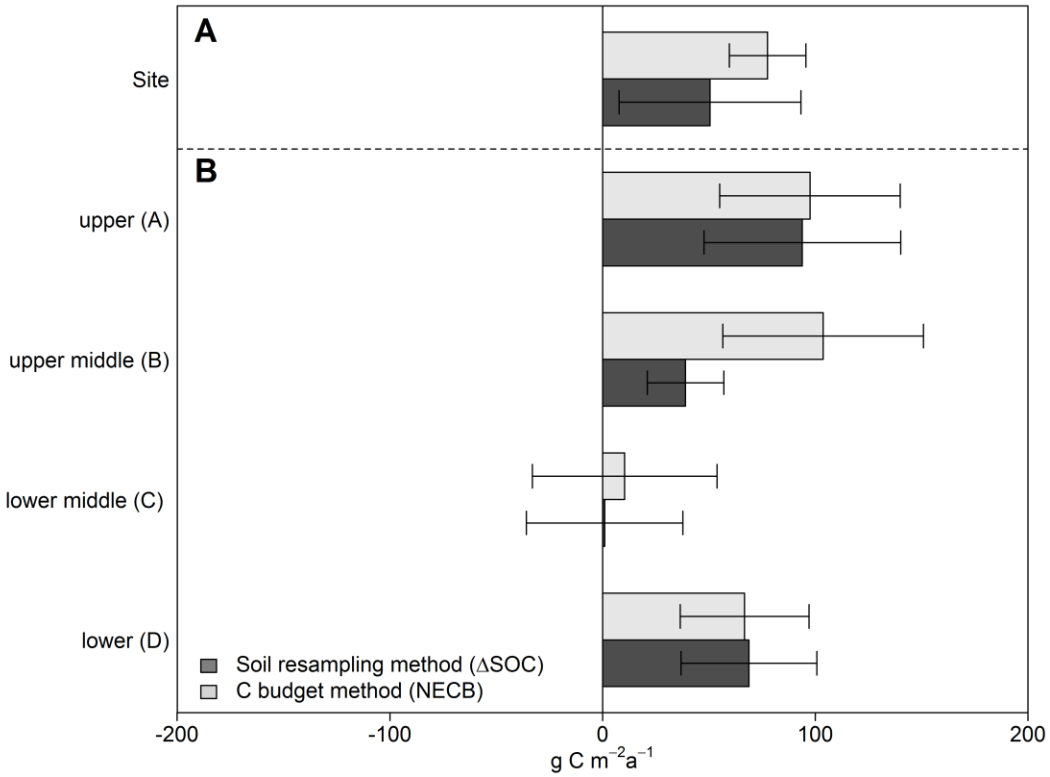

884

885

886

887

888

889

890

891

892

893

Appendices

A.1

Crop	Treatment	Details	Date
Winter fodder rye (*Secale cereale***)**	Chamber dismounting		10/04/2010
	Herbicide application	Roundup (2 l/ha)	19/04/2010
	Fertilization	KAS (160 kg/ha N), 110 kg/ha P2O5, 190 kg/ha K2O, 22 kg/ha S and 27 kg/ha MgO	23/04/2010
	Ploughing	Chisel Plough	23/04/2010
	Sowing	10 seeds/m^2	23/04/2010
Silage maize (*Zea mays***)**	Chamber installation		04/05/2010
	Herbicide application	Zintan Platin Pack	26/05/2010
	Harvest		19/09/2010
Bare soil	Chamber dismounting		20/09/2010
	Chamber installation		27/10/2010
	Chamber dismounting		05/04/2011
	Fertilization	110 kg/ha P2O5, 190 kg/ha K2O, 22 kg/ha S and 27 kg/ha MgO	06/04/2011
	Ploughing	Chisel Plough	21/04/2011
Silage maize (*Zea mays***)**	Sowing	10 seeds/m^2	21/04/2011
	Herbicide application	Gardo Gold Pack, 3.5 l/ha	27/04/2011
	Fertilization	KAS (160 kg/ha N)	03/05/2011
	Chamber installation		04/05/2011
	Harvest		13/09/2011
Bare soil	Chamber dismounting		13/09/2011
	Ploughing	Chisel Plough	30/09/2011
Winter fodder rye (*Secale cereale***)**	Sowing	270 seeds/m^2	30/09/2011
	Chamber installation		05/10/2011
	Fertilization	KAS (80 kg/ha N)	06/03/2012
	Harvest		02/05/2012
Bare soil	Chamber dismounting		02/05/2012
	Ploughing		08/05/2012
Sorghum-Sudan grass (*Sorghum bicolor* x *sudanese***)**	Sowing	30 seeds/m^2	09/05/2012
	Fertilization	KAS (100 kg/ha N), Kieserite (100 kg/ha), 220 kg/ha P2O5, 190 kg/ha K2O	14/05/2012
	Chamber installation		22/05/2012
	Replanting		29/05/2012
	Herbicide application	Gardo Gold Pack (3 l/ha), Buctril (1.5 l/ha)	12/07/2012
	Harvest		18/09/2012
Bare soil	Chamber dismounting		19/09/2012
	Ploughing	Chisel Plough	09/10/2012
Winter triticale (*Triticosecale***)**	Sowing	400 seeds/m^2	09/10/2012
	Chamber installation		19/10/2012
	Chamber dismounting		20/09/2012
	Chamber installation		17/10/2012
Luzerne (*Medicago sativa***)**	Ploughing; fertilization	Chisel Plough; 44 kg/ha K2O, 48.4 kg/ha P40	15/04/2013
	Sowing	22 kg/ha	18/04/2013
	Harvest (first cut)		04/07/2013
	Fertilization	88 kg/ha K2O	10/07/2013
	Harvest (second cut)		21/08/2013
	Fertilization	200 kg/ha K2O, 110 kg/ha P2O5	27/02/2014
	Harvest (first cut)		29/04/2014
	Harvest (second cut)		10/06/2014
	Harvest (third cut)		21/07/2014
	Harvest (fourth cut)		27/08/2014
	Chamber dismounting		28/08/2014

A.2 Weather and soil conditions

A.3 shows the development of important environmental variables throughout the study period (January 2010 – December 2014). In general, weather condition were similarly warm (8.7°C) but also wetter (562 mm) compared to the long-term average (8.6°C; 485 mm). Temperature and precipitation were characterized by distinct inter- and intra-annual variability. The highest annual air temperature was measured in 2014 (9°C). The highest annual precipitation was recorded during 2011 (616 mm). Lower annual mean air temperature and comparatively drier weather conditions were recorded in 2010 (7.7°C; 515 mm) and 2013 (8.5°C; 499 mm). Clear seasonal patterns were observed for air temperature. The daily mean air temperature at a height of 200 cm varied between -18.8°C in February 2012 and 26.3°C in July 2010. Rainfall was highly variable and mainly occurred during the growing season (55 % to 93 %), with pronounced heavy rain events during summer periods, exceeding 50 mm d^{-1}. Despite a rather wet summer, only 67 mm was measured in March and April 2012, the driest spring period within the study, resulting in late germination and reduced plant growth. Annual GWL differed by up to 77 cm along the chamber transect and followed precipitation patterns. Seasonal dynamics were characterized by a lower GWL within the growing season (1.10 m) and enhanced GWL during the non-growing season (0.85 m). From a short-term perspective, GWL was closely related to single rainfall events. Hence, a GWL of 0.10 m was measured immediately after a heavy rainfall event in July 2011, whereas the lowest GWL occurred during the dry spring in 2010. From August 2013 to December 2014, the GWL was too low to apply the principal of hydrostatic equilibrium; therefore, the groundwater table depth (> 235 cm) had to be used as a proxy.

A.3

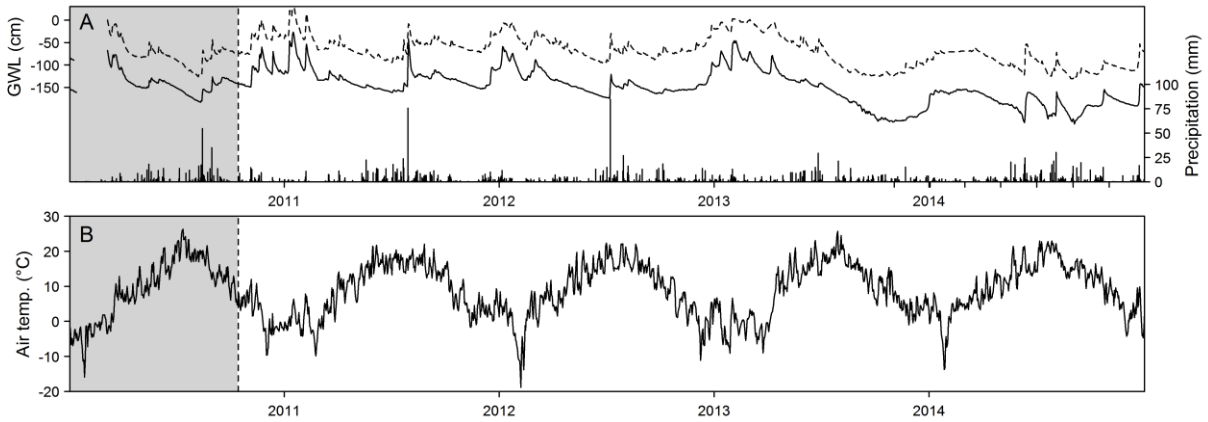
A
GWL (cm)
0
-50
-100
-150
Precipitation (mm)
100
75
50
25
0
2011
2012
2013
2014
B
Air temp. (°C)
30
20
10
0
-10
-20
2011
2012
2013
2014